# The Temperature-Dependence of Hydrophobic Association in Water. Pair versus Bulk Hydrophobic Interactions

**Susanna Lüdemann,*,† Roger Abseher,† Hellfried Schreiber, and Othmar Steinhauser**

*Contribution from the Institut für Theoretische Chemie, Theoretical Biochemistry Group Universität Wien, Währinger Strasse 17, A-1090 Wien, Austria*

*Received October 12, 1995. Revised Manuscript Received February 20, 1997*[⊗]

**Abstract:** The temperature dependence of hydrophobic interactions of methane-like particles in water is analyzed in terms of free energy, entropy, internal energy, and the second osmotic virial coefficient. A large computational effort (approximately 15 ns cumulative trajectory length at each temperature) has been undertaken in order to guarantee reliable free energy and entropy data. At 300 K association is controlled by entropy, but as the temperature rises the internal energy takes over and dominates at 500 K. Both internal energy and entropy change sign within this temperature range. Our results correspond qualitatively with the experimentally observed temperature effect for transfer of gaseous hydrophobic substances into water: $\Delta A$ shows a weak temperature dependence, while $\Delta E$ and $\Delta S$ vary strongly with temperature. The second osmotic virial coefficients were calculated at different temperatures. Agreement with osmotic virial coefficients measured by solubility experiments at 300 K was found. Our results indicate that pairwise hydrophobic association studied by molecular dynamics simulation shows the key effects reported for bulk hydrophobic interactions. At present, there is no evidence for a qualitative difference between pair and bulk hydrophobic interactions. It is demonstrated that the comparison of the second osmotic virial coefficient of the solute particles in water, $B_{2,aq}$, with that in the pure gas phase, $B_{2,g}$, is not apppropriate for an assessment of the influence of water on pairwise hydrophobic interactions.

## 1. Introduction

The characteristic behavior of two or more nonpolar particles or residues in water is generally described as a "hydrophobic interaction".[1−3] This hydrophobic interaction is the key effect responsible for the immiscibility of water and nonpolar liquids as well as for such biologically important processes as the self-assembly of biological membranes.[4] It is widely considered as the driving force in protein folding, although this view has been criticized.[5,6] Hydrophobic interactions involve an indirect solvent-mediated component,[7−16] which is considered to result from the peculiar water structure at nonpolar surfaces.

Commonly, a distinction is made between pairwise and bulk hydrophobic interactions in water. Bulk hydrophobic interactions in water involve "large clusters of nonpolar groups as may, for instance, be found in the interior of a protein molecule".[17] Pairwise hydrophobic interactions instead refer to two nonpolar particles and have been described as qualitatively different from bulk hydrophobic interactions.[18]

Bulk hydrophobic interactions in water have been experimentally characterized by transfer experiments of nonpolar substances to water.[6] Transfer from a neat hydrophobic phase to an aqueous phase at room temperature is accompanied by a favorable enthalpic contribution, which is smaller in magnitude than the unfavorable entropy. The transfer heat capacity change is large and positive and responsible for the inversion of the roles of entropy and enthalpy, i.e., both of them change sign, as the temperature is increased.

Pairwise hydrophobic interactions in aqueous solution are much less amenable to experimental methods. A quantity often used to describe their strength is the second osmotic virial coefficient ($B_2$ ).[19−21] It is an integral measure of the association tendency of two solute molecules in water compared with the association tendency in a random solution. The more negative $B_2$, the stronger the association tendency. Both experimentalists and theoreticians have come upon the puzzling finding that small hydrophobic particles in aqueous solution show a second osmotic virial coefficient close to zero.[9,22] This has led to the notion of "hydrophobic repulsion".[9,22] Comparison of the second osmotic virial coefficient of the solute particles in water, $B_{2,aq}$, with that in the pure gas phase, $B_{2,g}$, has led to the conclusion that water weakens pairwise hydrophobic interac-

* Corresponding author, e-mail: Susanna.Luedemann@embl-heidelberg.de.

† Present address: European Molecular Biology Laboratory, Meyerhofstrasse 1, D-69117 Heidelberg, Germany.

⊗ Abstract published in *Advance ACS Abstracts,* April 15, 1997.

(1) Kauzmann, W. *Adv. Protein Chem.* **1959**, *14*, 1.
(2) Franks, F., E. *Water. A Comprehensive Treatise*; Plenum Press: New York, 1972−1982.
(3) Ben-Naim, A. *Statistical Thermodynamics for Chemists and Biochemists*; Plenum Press: New York, 1992.
(4) Tanford, C. *The Hydrophobic Effect*, John Wiley and Sons: New York, 2nd ed.; 1980.
(5) Ben-Naim, A. *Biopolymers* **1990**, *29*, 567.
(6) Privalov, P. L.; Gill, S. J. *Adv. Protein Chem.* **1988**, *39*, 191.
(7) Pratt, L.; Chandler, D. *J. Chem. Phys.* **1977**, *67*, 3683.
(8) Pangali, C.; Rao, M.; Berne, B. J. *J. Chem. Phys.* **1979**, *71*, 2982.
(9) Watanabe, K.; Andersen, H. C. *J. Phys. Chem.* **1986**, *90*, 795.
(10) Skipper, N. T. *Chem. Phys. Lett.* **1993**, *207*, 424.
(11) Smith, D. E.; Zhang, L.; Haymet, A. D. J. *J. Am. Chem. Soc.* **1992**, *114*, 5875.
(12) Smith, D. E.; Haymet, A. D. J. *J. Chem. Phys.* **1993**, *98*, 6445.
(13) van Belle, D.; Wodak, S. J. *J. Am. Chem. Soc.* **1993**, *115*, 647.
(14) New, M. H.; Berne, B. J. *J. Am. Chem. Soc.* **1995**, *117*, 7172−7179.
(15) Lüdemann, S.; Schreiber, H.; Abseher, R.; Steinhauser, O. *J. Chem. Phys.* **1996**, *104*, 286−295.
(16) Hummer, G.; Garde, S.; Garcia, A. E.; Pohorille, A.; Pratt, L. R. *Proc. Natl. Acad. Sci. U.S.A.* **1996**, *93*, 8951−8955.
(17) Kozak, J. J.; Knight, W. S.; Kauzmann, W. *J. Chem. Phys.* **1968**, *48*, 675−690.
(18) Wood, R. H.; Thompson, P. T. *Proc. Natl. Acad. Sci. U.S.A.* **1990**, *87*, 946.
(19) Yaacobi, M.; Ben-Naim, A. *J. Phys. Chem.* **1974**, *78*, 175.
(20) Tucker, E. E.; Christian, S. D. *J. Phys. Chem.* **1979**, *83*, 426.
(21) Tucker, E.; Lane, E. H.; D., C. S. *J. Solut. Chem.* **1981**, *10*, 1.
(22) Kennan, R. P.; Pollack, G. L. *J. Chem. Phys.* **1990**, *93*, 2724.

S0002-7863(95)03439-1 CCC: $14.00 

tions.[18] It is one of the aims of this paper to resolve this apparent contradiction.

Pioneering theoretical work on the pairwise hydrophobic effect has been performed by Pratt and Chandler.[7] Their theory is based on an integral equation for the pair correlation functions associated with spherical nonpolar species dissolved in water. It provides a framework for the study of hydrophobic association, that does not depend on a particular set of solute−solute and solute−water interaction parameters.

The concept of pairwise hydrophobic interaction adopted in the present computer simulations derives from microscopic liquid theory. It is defined as the solute−solute free energy of interaction obtained by integration over the solute−solvent and solvent-solvent degrees of freedom at a given intersolute distance.[23,24]

In a previous publication, the free energy of association of two methane-like particles and its increase with rising temperature was reported.[15] In the present study the potential of mean force is decomposed into its entropy and internal energy contribution. Until now a decomposition into entropy and internal energy has only been performed in a few molecular dynamics studies.[12,25,26] We further show that simulation reproduces the inversion of the roles of entropy and internal energy for hydrophobic association with increasing temperature. We relate our results to both experimental transfer data as well as to second osmotic virial coefficients of aqueous solutions of hydrophobic compounds. At least qualitative agreement is found in both cases. At the same time, we emphasize that free energy and second osmotic virial coefficients are neither equivalent nor easily comparable measures of hydrophobicity.

## 2. Theory

**Free Energy.** The potential of mean force for the association of two methane-like particles in water was calculated as described previously[15] by the perturbation method and the thermodynamic integration method.[27,23] The total energy of association is defined as

$$\Delta A_{tot}(r) = \Delta A_{ind}(r) + E_{LJ}^{SS}(r) \tag{1}$$

where $r$ is the solute−solute separation, $\Delta A_{ind}(r)$ is the solvent-mediated free energy of association, and $E_{LJ}^{SS}(r)$ is the direct Lennard−Jones interaction potential of the two solutes that is not subject to configurational averaging.[15] $\Delta A_{ind}(r)$ is calibrated in such a way that $\Delta A_{ind}(r_{max})$ equals zero. $r_{max}$ is the maximum solute−solute distance that has been considered.

**Entropy.** Different methods for calculating entropy and internal energy from MD have been reported.[11,12,28−32]

In this study two different methods for the calculation of the solvent-mediated entropy of association $\Delta S_{ind}$ have been applied: (1) The entropy was calculated from the free energy at two temperatures via the finite difference temperature derivative:[12]

$$-\Delta S_{ind}(r,T) \approx \frac{1}{2\Delta T}(\Delta A_{ind}(r, T + \Delta T) - \Delta A_{ind}(r, T - \Delta T)) \tag{2}$$

(2) The thermodynamic integration method[11,12] has been applied. $\Delta S_{ind}(r)$ is then given by

$$-T\,\Delta S_{ind}(r) = 1/kT \int_{r_{max}}^{r} dR\left[\left\langle E(R)\frac{\partial E(R)}{\partial R}\right\rangle - \langle E(R)\rangle\left\langle\frac{\partial E(R)}{\partial R}\right\rangle\right] \tag{3}$$

**Second Osmotic Virial Coefficient.** We calculated partial integrals of the second osmotic virial coefficient

$$B_2(r) = -2\pi\int_0^r r'^2[g(r') - 1]dr' \tag{4}$$

and $B_2 = \lim_{r\to\infty} B_2(r)$ approximated by $B_2(r_{max})$. $g(r) = \exp(-\Delta A_{tot}(r)/RT)$ is the radial pair correlation function.

## 3. Methods

**MD-Simulations.** The simulations have been carried out with a program package written by the authors using the GROMOS topology and forcefield. Long-range electrostatics are treated by Ewald summation.[33−35]

The simulated system consists of two nonpolar methane-like solute atoms and 516 SPC water molecules in a cubic box 2.5 × 2.5 × 2.5 nm in size. According to the minimum image convention solute−solute separations up to 1.25 nm could be studied. When the temperature was increased, a system density of 0.991 g/mL was mantained.[15] Temperature was kept at its respective reference value by coupling the system to a heat bath.[36] Further simulation details are given in ref 15.

**Variation of Lennard−Jones parameters.** The GROMOS forcefield describes the Lennard−Jones interactions as pairwise additive and spherically symmetric:

$$U_{ab}(r) = 4\epsilon_{ab}\left[\left(\frac{\sigma_{ab}}{r}\right)^{12} - \left(\frac{\sigma_{ab}}{r}\right)^{6}\right] \tag{5}$$

We have applied two different sets of Lennard−Jones parameters for the interaction between the nonpolar solute and the water oxygen in conjunction with various solute−solute parameters (cf. Table 1). A CH1-like and a CH3-like solute in terms of the GROMOS87 forcefield[37] have been considered in order to investigate the parameter dependence of $B_2$. Further discussion of the choice of the parameters is given in ref 15. As the intersolute distance is restrained, no direct intersolute interactions are acting during the simulations. The advantage of this procedure is that one is free to choose the Lennard−Jones solute−solute interaction parameters after the simulations have been accomplished. It has been pointed out, however, that consistency of the parameters is essential.[15]

**Free Energy, Entropy and Internal Energy.** Methodological details for the calculation of the free energy are given elsewhere.[15] Free energy data served as an input for the calculation of the entropy, $\Delta S_{ind}(r)$, by the finite difference method. The applicability of the finite difference temperature derivative (eq 2) relies on the assumption that $\Delta C_V$ is temper-

(23) Beveridge, D. L.; DiCapua, F. M. *Annu. Rev. Biophys. Biophys. Chem.* **1989**, *18*, 431.
(24) Straatsma, T. P.; McCammon, J. A. *Annu. Rev. Phys. Chem.* **1992**, *41*, 407.
(25) Head-Gordon, T. *Chem. Phys. Lett.* **1994**, *227*, 215.
(26) Head-Gordon, T. *J. Am. Chem. Soc.* **1995**, *117*, 501.
(27) van Gunsteren, W. F.; Weiner, P. K. *Computer Simulation of Biomolecular Systems*; Leiden: ESCOM, 1989.
(28) Guillot, B.; Guissani, Y.; Bratos, S. *J. Chem. Phys.* **1991**, *95*, 3643.
(29) Brooks III, C. *J. Phys. Chem.* **1986**, *90*, 6680.
(30) Fleischman, S. H.; Brooks III, C. *J. Chem. Phys.* **1987**, *87*, 3029.
(31) Mezei, M.; Beveridge, D. L. *Ann. N. Y. Acad. Sci.* **1986**, *482*, 3643.
(32) Chialvo, A. A. *J. Chem. Phys.* **1990**, *92*, 673.
(33) Ewald, P. P. *Ann. Phys.* **1921**, *64*, 253.
(34) de Leeuw, S. W.; Perram, J. W.; Smith, E. R. *Proc. R. Soc. Lond., A* **1980**, *373*, 27−56.
(35) Adams, D. J.; Dubey, G. S. *J. Comput. Phys.* **1987**, *72*, 156−176.
(36) Berendsen, H. J. C.; Postma, J. P. M.; DiNola, A.; Haak, J. R. *J. Chem. Phys.* **1984**, *81*, 3684−3690.
(37) van Gunsteren, W. F.; Berendsen, H. J. C., *GROningen MOlecular Simulation (GROMOS) library manual*; Biomos: Groningen, The Netherlands, 1987.

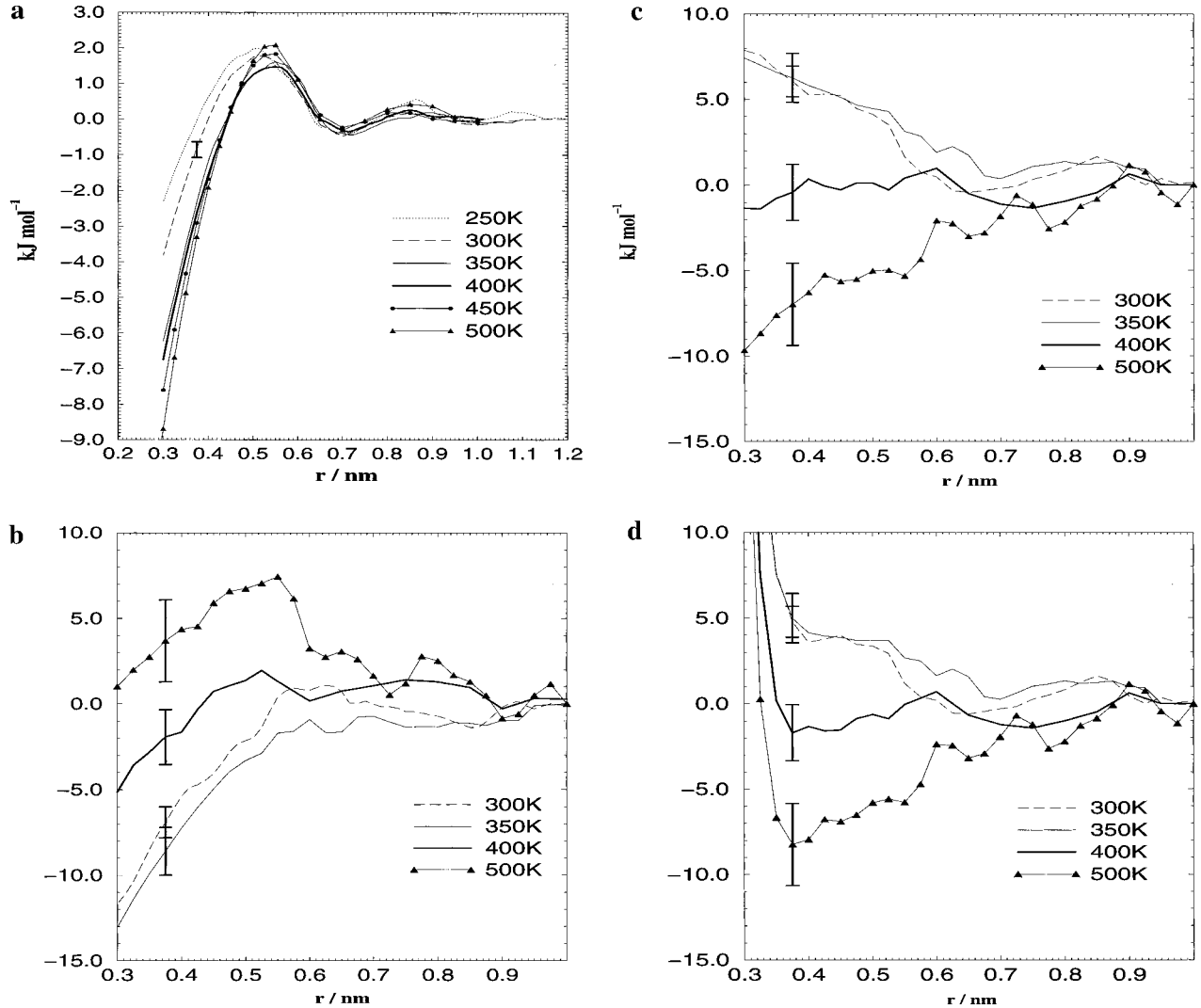


**Figure 1.** Free energy, entropy and internal energy of cavity association as a function of temperature at constant density. (a) The hydrophobic association monitored by $\Delta A_{ind}(r)$ increases with rising temperature, predominantly in the range of 250−350 K. (b) $-T\Delta S_{ind}(r)$. For 300, 350, and 400 K hydrophobic association is entropy-driven. At 500 K the entropical contribution to $\Delta A_{ind}(r)$ becomes unfavorable for association. (c) Internal energy $\Delta E_{ind}(r)$. It is unfavorable for association at 300 and 350 K, indifferent at 400 K, and becomes responsible for association at 500 K. (d) $\Delta E_{tot}(r)$ including the contribution of the direct methane−methane interaction at different temperatures. $\Delta E_{tot}(r)$ is positive for all separations at 300 K, while at 400 and 500 K a minimum occurs at the contact distance. The parameters for direct solute−solute interaction are $\sigma_{SS} = 3.57$ Å and $\epsilon_{SS} = 0.4$ kcal mol$^{-1}$. Error bars ($\pm 2\sigma$ ) representing the statistical error at contact distance are included in each Figure. The error is smaller for larger solute−solute separations (cf. Figure 2b).

ature independent within the temperature interval considered. For a temperature interval of 100 K the heat capacity difference for transfer of methane to water is approximately constant.[6] In the present study values of $\Delta T = 50$ K (300, 350, 400 K) and $\Delta T = 25$ K (325, 375 K) as defined in eq 2 were used. As the temperature dependence of $\Delta A_{ind}(r)$ decreases with rising temperature, it is not possible to get statistically significant finite difference temperature derivatives for 450 K. At 500 K $\Delta S_{ind}(r)$ was determined by the thermodynamic integration method. In addition the entropy at 300 K was also calculated by thermodynamic integration for comparison purposes. Trajectories of at least 500 ps for each intersolute separation are required in order to obtain reliable results. For 300 K 37 windows of 0.25 Å size were chosen, for 350 K 33, and for all other temperatures 29 windows. Consequently the total simulation effort for calculating the entropy is between 14.5 to 18.5 ns for each temperature value.

The internal energy was determined as $\Delta E_{ind} = \Delta A_{ind}(r) + T\Delta S_{ind}(r)$ for all temperatures. The total internal energy was decomposed into the contributions from solute−water (SW) and water−water (WW ) interactions. The uncertainty in the water−water configurational energy of the total system is too large for a reliable determination of $\Delta E_{WW}(r) = \langle E_{WW}(r)\rangle - \langle E_{WW}(r_{max})\rangle$. The solute−water energy $E_{SW}(r)$ is, however, a small quantity and shows fluctuations small enough for a reliable calculation of $\Delta E_{SW}(r)$:

$$\Delta E_{SW}(r) = \langle E_{SW}(r)\rangle - \langle E_{SW}(r_{max})\rangle \qquad (6)$$

This allows for an indirect determination of the water−water energy $\Delta E_{WW}(r)$ was obtained from

$$\Delta E_{WW}(r) = \Delta A_{ind}(r) + T\Delta S_{ind}(r) - \Delta E_{SW}(r) \qquad (7)$$

**Statistical Error Analysis.** The error in $\Delta A_{tot}(r)$ has been determined using the correlation analysis described by Straatsma et al.[40] The quality of the free energy data may also be estimated

(38) Jorgensen, W. L.; Madura, J. D.; Swenson, C. J. *J. Am. Chem. Soc.* **1984**, *106*, 6638.
(39) Allen, M. P.; Tildesley, D. J. *Computer Simulation of Liquids*; Clarendon Press: Oxford, 1987.
(40) Straatsma, T. P.; Berendsen, H. J. C.; Stam, A. J. *Mol. Phys.* **1986**, *57*, 89.

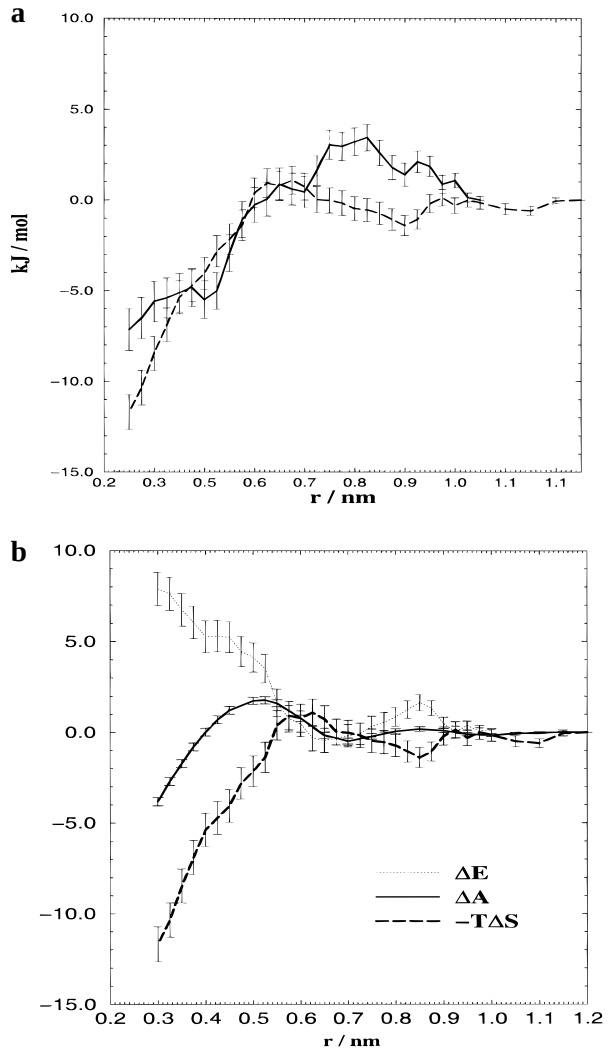


**Figure 2.** (a) $-T\Delta S_{ind}(r)$ at 300 K, calculated by different methods. (solid line, thermodynamic integration; dashed line, finite difference method). The error bars display the statistical errors ($\pm 2\sigma$ ) for each curve. The systematic errors inherent to the two different methods give rise to differences between the two curves that exceed the statistical errors on both of them. (b) The statistical error in $\Delta A_{ind}(r)$, $-T\Delta S_{ind}(r)$, and $\Delta E_{ind}(r)$ at 300 K.

from the comparison of the results obtained by perturbation and thermodynamic integration (cf. Figure 2 in ref 15). The systematic errors inherent to the present implementations of these two methods are not larger than the statistical error.

The statistical error in the entropy, the internal energy, and the second osmotic virial coefficient was determined using standard error propagation analysis. In contrast to the free energy, systematic errors in the entropy exceed statistical errors (cf. Figure 2a).

The errors shown in the present paper represent $\pm 2\sigma$ throughout.

## 4. Results

**4.1. Free Energy, Entropy, and Internal Energy.** The potential of mean force for two methane-like particles in water shows a stronger association of the particles with increasing temperature (cf. ref 15 and Figure 1a). $\Delta A_{ind}(r)$ displays the following features: A markedly temperature-dependent contact branch; an unfavorable solvent-bridged configuration, which is also referred to as desolvation barrier and displays a weaker and different temperature dependence; and two minima (around 0.7 and 1.0 nm) with even weaker temperature dependence, the second being very weak. All these features can be reproduced by an information theory model of the hydrophobic interaction put forward recently.[16]

$-T\Delta S_{ind}(r)$ for association of the solutes exhibits a stronger temperature dependence than the potential of mean force (cf. Figure 1b). $-T\Delta S_{ind}$ at 300 K is obtained as $-5.25 \pm 1.10$ kJ/mol (thermodynamic integration) and $-6.90 \pm 0.90$ kJ/mol (finite difference method), respectively, at solute contact (3.75 Å), indicating that association at this temperature is entropy-driven. This has also been reported by Smith and Haymet.[12] With increasing temperature the entropic contribution to $\Delta A_{ind}(r)$ decreases. At 500 K $-T\Delta S_{ind}$ is $+3.67 \pm 2.40$ kJ/mol at solute contact (3.75 Å) (cf. Table 2). At this temperature the entropy no longer favors association. The entropy would rather give rise to dissociation of the solute pair.

A comparison of $\Delta S_{ind}(r)$ obtained by the finite difference and the thermodynamic integration method is shown in Figure 2a.

It is the internal energy $\Delta E_{ind}(r)$ that dominates $\Delta A_{ind}(r)$ at 500 K. It becomes responsible for the association of the solutes at 500 K (cf. Figure 1c). Thus the roles of entropy and internal energy change completely in the interval from 300 to 500 K. $\Delta E_{tot}(r)$, the internal energy including direct solute interactions, is positive for all solute separations at 300 K and 350 K. At 400 K and 500 K a minimum at solute contact is observed (cf. Figure 1d).

The decomposition of $\Delta E_{ind}(r)$ into solute−water, $\Delta E_{SW}(r)$, and water−water contributions $\Delta E_{WW}(r)$, is displayed in Figure 3. The total internal energy of association and its temperature behavior is dominated by the water−water interactions.

An overview of the thermodynamic association data is given in Table 2.

In order to depict the inversion of the roles of entropy and internal energy with increasing temperature more clearly, $\Delta A_{ind}(r_{cp})$, $-T\Delta S_{ind}(r_{cp})$, and $\Delta E_{ind}(r_{cp})$ with $r_{cp} = 3.75$ Å are plotted vs temperature (cf. Figure 4).

**4.2. Second Osmotic Virial Coefficients.** As hydrophobic compounds hardly dissolve in water, direct experimental determination of the thermodynamics of association is rather difficult. To our knowledge only a few experiments have been carried out in this field.[20,21] Second osmotic virial coefficients are more frequently determined. For comparison, second osmotic virial coefficients have been calculated for two sets of solute−water interaction parameters, under variation of the solute−solute interaction parameters and for different temperatures.

**4.2.1. CH1-like Solute.** For parameter set 1 ($\sigma_{SO} = 3.336$ Å, $\epsilon_{SO} = 0.241$ kcal mol$^{-1}$), a negative $B_{2,aq}$ is observed, and agreement with experimental results available for temperatures close to 300 K[9,22] is found (cf. Table 3). $B_{2,aq}$ is negative at 300, 350, and 400 K. At 450 and 500 K positive values are observed (Table 3a). The second osmotic virial coefficients for the pure solute gas phase, $B_{2,g}$ have been calculated according to

$$B_{2,g} = -2\pi \int_0^\infty \{\exp(-E_{LJ}^{SS}(r)/RT) - 1\} \cdot r^2 dr \qquad (8)$$

with

$$E_{LJ}^{SS}(r) = 4\epsilon_{SS}\left[\left(\frac{\sigma_{SS}}{r}\right)^{12} - \left(\frac{\sigma_{SS}}{r}\right)^{6}\right] \qquad (9)$$

The parameters $\epsilon_{SS}$ and $\sigma_{SS}$ are the same as those used for the determination of the second osmotic virial coefficient in solution. $[B_{2,aq} - B_{2,g}]$ is considered as a measure of the influence water

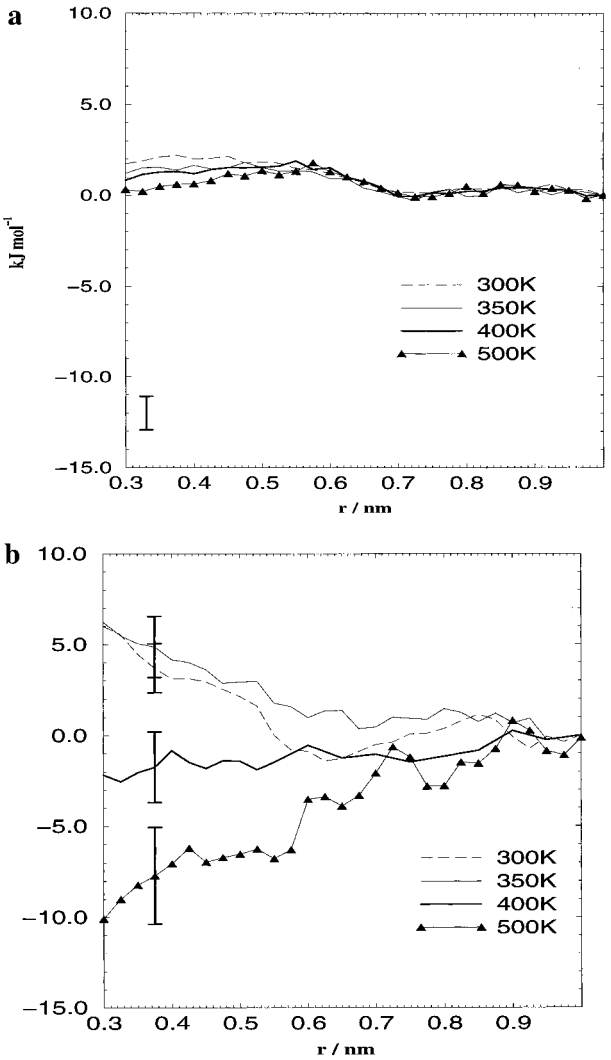


**Figure 3.** Decomposition of the internal energy, $\Delta E_{ind}(r)$, into (a) the solute−water $\Delta E_{SW}(r)$ and (b) the water−water contribution $\Delta E_{WW}(r)$. The density is 0.991 g/mL for all temperatures. The solute−water energy is small and not very sensitive to temperature. Thus the temperature dependence of the total internal energy, $\Delta E_{ind}(r)$, can be attributed to water effects. Error bars ($\pm 2\sigma$) representing the maximal statistical error are included.

exerts on pairwise hydrophobic interactions.[18,41] The difference $[B_{2,aq} - B_{2,g}]$ is small: The largest value found is at 300 K (89 ± 38 Å$^3$); at 350 K $[B_{2,aq} - B_{2,g}]$ is slightly negative (−18 ± 34 Å$^3$) and again becomes positive above 350 K. Following the argumentation of Wood and Thompson[18] this would mean that only at 350 K does water promote association.

If a smaller solute−solute dispersion $\epsilon_{SS}$ is used together with par.set1 we find a more positive $B_{2,aq}$: $B_{2,aq}$ is +69 ± 38 Å$^3$ for $\epsilon_{SS} = 0.1$ kcal mol$^{-1}$ ($T = 300$ K) (cf. Table 3a).

**4.2.2. CH3-like Solute.** Use of consistent solute−solute parameters ($\epsilon_{SS} = 0.718$ kcal mol$^{-1}$, $\sigma_{SS} = 3.235$ Å) together with par.set2 (cf. Table 1) yields a $B_{2,aq}$ of −10 ± 40 Å$^3$ ($T =$ 300 K). Comparing $B_{2,aq}$ and $B_{2,g}$ we get the following picture: Solute particles interacting more strongly with both the other solute and water yield a $B_{2,aq}$ (−10 ± 40 Å$^3$) that differs insignificantly from that obtained with par.set1 ($B_{2,aq} =$ −26 ± 38 Å$^3$, $T = 300$ K). $B_{2,g}$, however, is strongly affected and shifted toward more negative values. For par.set2 $B_{2,g}$ is found to be −248 Å$^3$ versus −115 Å$^3$ for par.set1 (cf. Table 3a). Therefore one could speculate that yet stronger solute−water and solute−solute interactions, as this is the case for higher hydrocarbons, may yield even larger differences of $[B_{2,aq} - B_{2,g}]$. This is corroborated by experimental data that indicate that $B_{2,g}$ drops off to much more negative values than $B_{2,aq}$ for hydrocarbons of increasing size.[41,18]

(41) Archer, D. G. *J. Phys. Chem.* **1989**, *93*, 5272.

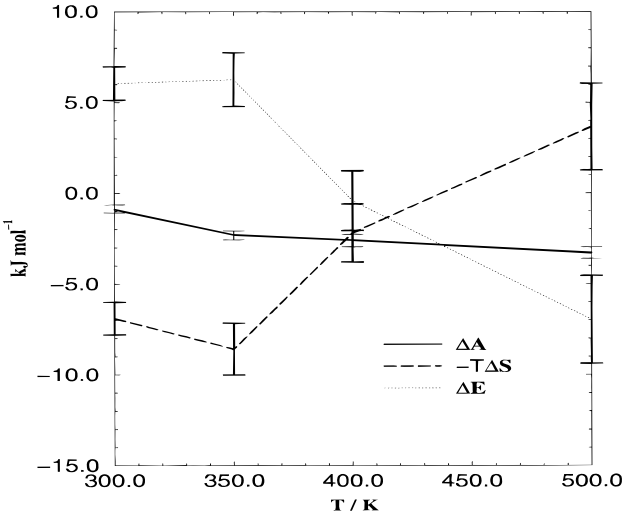


**Figure 4.** $\Delta A_{ind}(r_{cp})$, $-T\Delta S_{ind}(r_{cp})$, and $\Delta E_{ind}(r_{cp})$ as a function of temperature at constant density. The internal energy is found to change sign at around 400 K, while the entropy inverts in the interval between 400 and 450 K. $r_{cp}$ is the distance at which contact occurs, i.e., 3.75 Å. Error bars are drawn as $\pm 2\sigma$.

**Table 1.** Comparison of Solute−Water and Solute−Solute Lennard−Jones Parameters for Methane and CH1- and CH3-Groups in Proteins[a]

| solute−water | | solute−solute | | |
|---|---|---|---|---|
| $\sigma_{SO}$, Å | $\epsilon_{SO}$, kcal mol$^{-1}$ | $\sigma_{SS}$, Å | $\epsilon_{SS}$, kcal mol$^{-1}$ | solute specification |
| 3.336 | 0.241 | 3.57 | 0.1, 0.2, 0.3, **0.4** | CH1-like solute (par.set1) |
| 3.2 | 0.334 | 3.235 | 0.1, 0.2, 0.3, **0.718** | CH3-like solute (par.set2) |
| 3.4475 | 0.2134 | 3.73 | 0.2931 | $CH_4$[38] |
| 3.293 | 0.268 | 4.232 | 0.130 | CH1 (GROMOS87) |
| 3.115 | 0.315 | 3.79 | 0.180 | CH3 (GROMOS87) |
| 3.2 | 0.334 | 3.73 | 0.2931 | $CH_4$[7] |

[a] The solute−water parameter sets labeled par.set1 (all temperatures) and par.set2 (B2 at 300 K) are those actually used in the calculations. Consistent values (in terms of the Lorentz−Berthelot mixing rule[39]) of the solute−solute parameters applied are in boldface.

**4.3. Measures of Hydrophobicity.** The puzzling finding that the marked hydrophobic behavior of methane-like solutes concluded from the free energy data is not reflected in a similarly clear manner by the second osmotic virial coefficients requires a closer inspection of the underlying phenomena. In Figure 5 a comparison of the free energy of association in water and in the gaseous state is shown for 300 K.

At contact distance $\Delta A_{tot}$ (3.75 Å) is more negative than $E_{LJ}^{SS}$ (4.0 Å). In terms of free energy, hydrophobic association is *stronger* in water.

The calculation of second osmotic virial coefficients puts a strong weighting (proportional to $r^2$) on the values of $\Delta A_{tot}(r)$ at large solute−solute separations. The influence of the individual configurations on the second osmotic virial coefficient can be read from a plot of the partial integrals $B_2(r)$ shown in Figure 6. It illustrates the integration process yielding $B_2$. Partial integrals have been used in a parallel case in order to monitor the contributions of the solute−solvent radial distribution to the partial molar volume of the solute (cf. Figure 3 in ref 42).

**Table 2.** Methane Association Thermodynamics in the Interval between 300 and 500 K at Constant Density[a]

| *T*, K | $\Delta A_{ind}(r_{cp})$, kJ/mol | $-T\Delta S_{ind}(r_{cp})$, kJ/mol | $\Delta S_{ind}(r_{cp})$, J/(mol·K) | $\Delta E_{ind}(r_{cp})$, kJ/mol | $\Delta E_{SW}(r_{cp})$, kJ/mol | $\Delta E_{WW}(r_{cp})$, kJ/mol | $\Delta E_{tot}(r_{cp})$, kJ/mol |
|---|---|---|---|---|---|---|---|
| 300 | $-0.86 \pm 0.22$ | $-6.90 \pm 0.90$ (f.d.) | $23.0 \pm 3.0$ (f.d.) | $6.05 \pm 0.92$ (f.d.) | $2.04 \pm 0.96$ | $4.00 \pm 1.34$ (f.d.) | $4.78 \pm 0.92$ (f.d.) |
| | | $-5.25 \pm 1.10$ (t.i.) | $17.5 \pm 3.6$ (t.i.) | $4.39 \pm 1.12$ (t.i.) | | $2.34 \pm 1.48$ (t.i.) | $3.11 \pm 1.12$ (t.i.) |
| 325 | | $-9.91 \pm 2.12$ (f.d.) | $30.5 \pm 6.6$ (f.d.) | | | | |
| 350 | $-2.33 \pm 0.24$ | $-8.59 \pm 1.42$ (f.d.) | $24.5 \pm 4.0$ (f.d.) | $6.26 \pm 1.44$ (f.d.) | $1.40 \pm 0.88$ | $4.86 \pm 1.68$ (f.d.) | $4.98 \pm 1.44$ (f.d.) |
| 375 | | $-2.20 \pm 3.12$ (f.d.) | $5.9 \pm 8.4$ (f.d.) | | | | |
| 400 | $-2.62 \pm 0.34$ | $-2.20 \pm 1.60$ (f.d.) | $5.5 \pm 4.0$ (f.d.) | $-0.42 \pm 1.64$ (f.d.) | $1.32 \pm 1.04$ | $-1.74 \pm 1.94$ (f.d.) | $-1.70 \pm 1.64$ (f.d.) |
| 500 | $-3.30 \pm 0.32$ | $3.67 \pm 2.40$ (t.i.) | $-7.3 \pm 4.8$ (t.i.) | $-6.97 \pm 2.42$ (t.i.) | $0.66 \pm 1.10$ | $-7.63 \pm 2.66$ (t.i.) | $-8.24 \pm 2.42$ (t.i.) |

[a] Results have been obtained by the finite difference temperature derivative (f.d.) and the thermodynamic integration (t.i.) method. $r_{cp}$ is the distance at which contact association occurs, i.e., 3.75 Å. Errors are given as $\pm 2\sigma$.

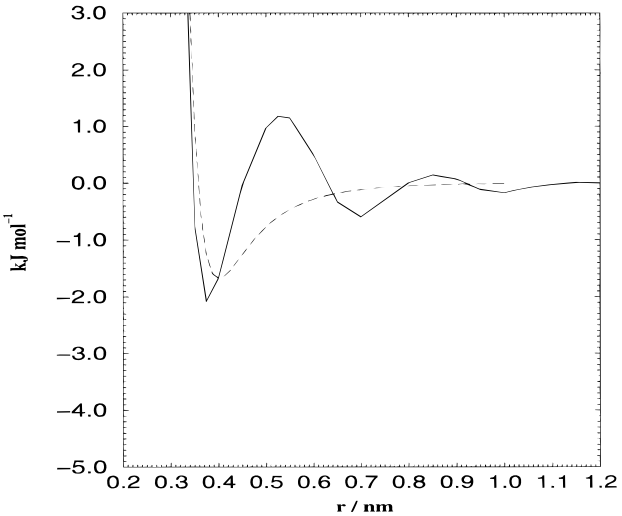


**Figure 5.** Comparison of the free energy of association of methane-like particles (par.set2) in water, $\Delta A_{tot}(r)$ (continuous line) and in the pure gaseous state, $E_{LJ}^{SS}(r)$ (dashed line). $\epsilon_{SO} = 0.241$ kcal mol$^{-1}$, $\sigma_{SO} = 3.336$ Å, $\epsilon_{SS} = 0.4$ kcal mol$^{-1}$, $\sigma_{SS} = 3.57$ Å, $T = 300$ K.

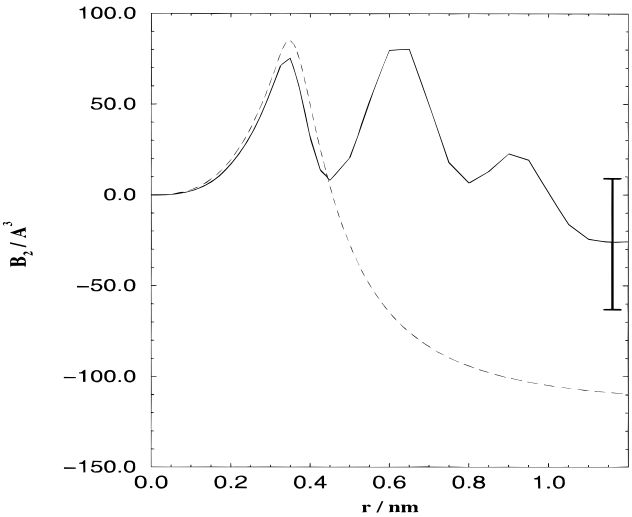


**Figure 6.** $B_{2,aq}(r)$ and $B_{2,g}(r)$. The absence of the solvent-bridged configuration in the gaseous state gives rise to the low values of $B_{2,g}$. $B_{2,aq}(r)$, continuous line; $B_{2,g}(r)$, dashed line; $T = 300$ K.

The contact and solvent-separated configuration give rise to negative increments of $B_{2,aq}(r)$ and are responsible for the minima of $B_{2,aq}(r)$ (cf. Figure 6). The height of the desolvation barrier strongly influences $B_{2,aq}$ and shifts it toward more positive values.

In terms of $B_2$ then we find an association "weakened by the influence of water".[18] This is in apparent contradiction to the free energy data. The free energy of association is the difference in free energy between contact pair and a pair of solutes at infinite distance, no matter what happens at other solute−solute separations. The second osmotic virial coefficient in water $B_{2,aq}$, however, is an integral quantity and is strongly influenced by the free energy values of the solvent-bridged configurations. Owing to the absence of solvent-bridged configurations in the gaseous state the direct comparison of $B_{2,aq}$ and $B_{2,g}$ is biased.

## 5. Discussion

**Association vs Dissolution Thermodynamics.** The temperature effect observed for $\Delta A_{ind}(r)$, $-T\Delta S_{ind}(r)$, and $\Delta E_{ind}(r)$ is qualitatively the same as that reported for the experimentally determined thermodynamic quantities of transfer. Transfer experiments record the thermodynamics of the transition from pure gas (g) or liquid (l) solute phase to solute dissolved in water (w).[6] The corresponding thermodynamic quantities are $\Delta_g^w G$, $-T\cdot\Delta_g^w S$, and $\Delta_g^w H$. Transfer of solute to water is commonly decomposed into the following processes:[44]

− the formation of a cavity in the water phase,

− the insertion of the apolar solute and the onset of the solute−water interaction,

− the restructuring of the water shell around the solute.

All three contributions are involved in the association of solutes in water although to a smaller extent and with opposite sign: (i) Instead of the creation of a new cavity, the solvent-accessible surface of the cavity in water is reduced upon association of the solute particles. For the contact pair, there is a nonvanishing fraction of the solute surface that is not accessible to the solvent. (ii) The onset of the solute−water interaction has its counterpart in the reduction of the number of solute−water interactions when association takes place. (iii) Restructuring of the newly created shell as a part of transfer experiments corresponds to restructuring around the contact pair. One has to bear in mind that this decomposition is undoubtly artificial. It is an attempt to decompose a single process into sequential steps for which no thermodynamic data can be obtained.

Owing to this analogy a similar temperature behavior as observed in transfer studies is plausible to occur for association. Comparison with experimental solubility data for methane in water at different temperatures[45,46] reveals the following similarities: (i) The Gibbs free energy of transfer shows a weak temperature dependence in comparison to the temperature dependence of its enthalpic and entropic components. We report

(42) Pratt, L. R.; Pohorille, A. Hydrophobic effects from cavity statistics. In *Association of European Biophysical Societies Conference Proceedings on Water-Biomolecule Interactions*; Palma, M. U., Palma-Vittorelli, M. B., Eds.; Bologna, Italy, 1992; Vol. 43, pp 261−268.

(43) Pratt, L. R.; Chandler, D. *J. Chem. Phys.* **1980**, *73*, 3434.

(44) Blokzijl, W.; Engberts, J. B. F. N. *Angew. Chem., Int. Ed. Engl.* **1993**, *32*, 1545.

(45) Crovetto, R.; Fernandez-Prini, R.; Japas, M. L. *J. Chem. Phys.* **1982**, *76*, 1077.

(46) Rettich, T. H.; Handa, Y. P.; Battino, R.; Wilhelm, E. *J. Phys. Chem.* **1981**, *85*, 3231.

**Table 3.** Comparison of Second Osmotic Second Virial Coefficients for Methane Respectively Methane-like Solutes Obtained by Simulation[b] (a) and Experiment (b)

(a)

| simulation | temp, K | $B_2$, Å$^3$ | LJ parameters |
|---|---|---|---|
| this study (aq) | 300 | $-26 \pm 38$ ($+69 \pm 38$) | $\epsilon_{SO} = 0.241$ kcal mol$^{-1}$, $\sigma_{SO} = 3.336$ Å |
| | 350 | $-103 \pm 34$ ($-26 \pm 34$) | (par.set1) |
| | 400 | $-50 \pm 34$ ($+13 \pm 34$) | $\epsilon_{SS} = 0.4(0.1)$ kcal mol$^{-1}$, $\sigma_{SS} = 3.57$ Å |
| | 450 | $+30 \pm 28$ ($+71 \pm 28$) | |
| | 500 | $+22 \pm 24$ ($+50 \pm 24$) | |
| this study (gas) | 300 | $-115$ ($+30$) | $\epsilon_{SS} = 0.4(0.1)$ kcal mol$^{-1}$, $\sigma_{SS} = 3.57$ Å |
| | 350 | $-85$ ($+35$) | |
| | 400 | $-60$ ($+40$) | |
| | 450 | $-45$ ($+40$) | |
| | 500 | $-30$ ($+45$) | |
| this study (aq) | 300 | $-10 \pm 40$ ($+176 \pm 40$) | $\epsilon_{SO} = 0.334$ kcal mol$^{-1}$, $\sigma_{SO} = 3.2$ Å |
| | | | (par.set2, [43]) |
| | | | $\epsilon_{SS} = 0.718(0.1)$ kcal mol$^{-1}$, $\sigma_{SS} = 3.235$ Å |
| this study (gas) | 300 | $-248$ ($+23$) | $\epsilon_{SS} = 0.718(0.1)$ kcal mol$^{-1}$, $\sigma_{SS} = 3.235$ Å |
| this study (aq) | 300 | $+156 \pm 40$ | $\epsilon_{SO} = 0.334$ kcal mol$^{-1}$, $\sigma_{SO}$) $= 3.2$ Å |
| | | | (par.set2,[43]) |
| | | | $\epsilon_{SS} = 0.2931$ kcal mol$^{-1}$, $\sigma_{SS} = 3.73$ Å[43] |
| this study (gas) | 300 | $-64$ | $\epsilon_{SS} = 0.2931$ kcal mol$^{-1}$, $\sigma_{SS} = 3.73$ Å |
| results from ref 12 | 298 | $-48$ | $\epsilon_{SO} = 0.2134$ kcal mol$^{-1}$, $\sigma_{SO} = 3.4475$ Å |
| | | | $\epsilon_{SS} = 0.2931$ kcal mol$^{-1}$, $\sigma_{SS} = 3.73$ Å[38] |

(b)

| experiment | temp, K | $B_2$, Å$^3$ |
|---|---|---|
| results from ref 22 | 298 | $+10$[a] |
| | | $-186$[a] |
| results from ref 9 | 298 | $-33$ |
| | 311 | $-118$ |

[a] The authors of ref 22 emphasize that the values they obtain for $B_2$ strongly depend on the partial molar volume data of the solute used. [b] $B_2$ data in brackets correspond to interaction parameters in brackets. Errors are given as $\pm 2\sigma$.

a similar finding for the free energy of association in our system (cf. Figure 4). (ii) Both entropy and enthalpy of transfer display a strong temperature dependence, which is also found for the temperature behavior of our simulated association data. Obviously, the corresponding temperature derivatives have opposite signs. In the case of the internal energy respectively enthalpy the analogy goes even further. The transfer enthalpy $\Delta_g^W H$ changes from negative to positive values within 350 and 400 K, which corresponds well with the inversion of sign found for $\Delta E_{ind}$ (3.75 Å) in the same temperature interval.[45]

A unifying scheme for the description of the thermodynamics of solvent reorganization associated with a physical or chemical process has been put forward by Grunwald et al.[47] Following their thermodynamic theory both transfer and association can be decomposed into a nominal (*nom*) and an environmental (*env*) reaction, the latter involving the solvent only. The environmental reaction, accounting for the solvent reorganization, is shown to be accompanied by a vanishing change in free energy, but nonvanishing changes of internal energy and entropy. This is termed enthalpy−entropy compensation. In fact, in our study we find that at all temperatures apart from 400 K the entropic and enthalpic contributions to the free energy of association are much larger than the free energy itself, which gives evidence of compensation. Furthermore, as $\Delta E_{WW}(r_{cp}) \gg \Delta E_{SW}(r_{cp})$ and $\Delta E_{env} \gg \Delta E_{nom}$ (in water, cf. ref 47) we may consider $\Delta E_{WW}(r_{cp})$ as an estimate of $\Delta E_{env}$, neglecting a contribution of $\Delta E_{SW}(r_{cp})$ to $\Delta E_{env}$. Using a statistical mechanics approach the temperature behavior of small molecule hydration has recently been explained in a compelling way.[48] An information theory model that employs properties of neat water alone[49] accounts for both hydrophobic hydration and association[16] and yields a quantitative description of the temperature dependence of the hydrophobic hydration entropy.[48]

An interesting finding reported by Head−Gordon[26] shows that not only the variation of temperature but also of the interaction length $\sigma_{SO}$ gives rise to a change of roles for the internal energy and entropy. It should be noticed, however, that in this study[26] neither the results for the free energy nor those for entropy and internal energy correspond with the data reported by Smith and Haymet,[12] who did MD-simulations with one of the parameter sets compared in ref 26. This could be due to the short sampling of approximately 100 ps reported[26] for the internal energy, while Smith and Haymet performed an averaging on the nanosecond time scale for each solute separation.

**Free Energy vs Second Osmotic Virial Coefficient.** Owing to the lack of a direct experimental characterization of hydrophobic association, the second osmotic virial coefficient is the key quantity for probing pairwise hydrophobic interaction. The second osmotic virial coefficient is a weighted integral of the potential of mean force, which is the very quantity characterizing pairwise hydrophobic association. There is an unequivocal procedure for the conversion of the free energy of association into the second osmotic virial coefficient but not in the opposite direction. A comparison of the total free energy of association in water, i.e. the sum of water-mediated and direct interactions, with the free energy of association in the pure gas phase indicates that water *increases* the association tendency of methane-like particles. Reassessment of the same problem with a different instrument, viz., the second osmotic virial coefficient as done by Wood and Thompson,[18] yields a different result: water may weaken the association tendency. These findings can unambiguously be attributed to the desolvation barrier which displays a positive free energy in water and does not occur in

(47) Grunwald, E.; Steel, C. *J. Am. Chem. Soc.* **1995**, *117*, 5687.
(48) Garde, S.; Hummer, G.; Garcia, A. E.; Paulaitis, M. E.; Pratt, L. R. *Phys. Rev. Lett.* **1996**, *77*, 4966−4968.
(49) Berne, B. J. *Proc. Natl. Acad. Sci. U.S.A.* **1996**, *93*, 8800−8803.

vacuo. Thus the second osmotic virial coefficient should be used with care when assessing hydrophobicity. A small positive virial coefficient does not necessarily indicate a tendency to solvation instead of association.

**Pair vs Bulk Interactions.** For a qualitative assessment of the influence of solvent on the association of hydrophobic particles a thermodynamic cycle[18,44] is used. The central argument[18] is that the transfer of an aggregate of $N$ hydrophobic particles from the pure gas phase into an aqueous solution is more favorable than the transfer of $N$ separate particles. Following this reasoning it is by no means obvious why there should be a qualitative difference between the case $N = 2$ and large $N$. It is only the use of the second osmotic virial coefficient for the characterization of hydrophobicity that gives rise to an apparent contradiction. Therefore, at present stage there is no proof for a qualitative difference between hydrophobic pair and bulk interactions.

**Acknowledgment.** The authors thank Rebecca Wade for valuable comments on the manuscript.

JA953439D